Available online at www.eccomasproceedia.org
Eccomas Proceedia COMPDYN (2021) 899-912

ECCOMAS
Proceedia

COMPDYN 2021
8th ECCOMAS Thematic Conference on
Computational Methods in Structural Dynamics and Earthquake Engineering
M. Papadrakakis, M. Fragiadakis (eds.)
Streamed from Athens, Greece, 28 - 30 June 2021

# LOCAL EFFECTS DUE TO THE SEISMIC INTERACTION BETWEEN INNVATIVE DUCTILE MASONRY INFILLS AND RC ELEMENTS

**Riccardo R. Milanesi[1], Valentino Bolis[2], Simone Pelucco[2], Paolo Morandi[3], Guido Magenes[1], Marco Preti[2]**

[1] University of Pavia, D.I.C.Ar.
via Ferrata 3, 27100, Pavia (PV), Italy
riccardo.milanesi@unipv.it , guido.magenes@unipv.it

[2] University of Brescia, D.I.C.A.T.A.M.
via Branze 43, 25123, Brescia (BS), Italy
valentino.bolis@unibs.it , s.pelucco@unibs.it , marco.preti@unibs.it

[3] Eucentre
via Ferrata 1, 27100, Pavia (PV), Italy
paolo.morandi@eucentre.it

## Abstract

*The seismic vulnerability of rigidly attached masonry infills has been repeatedly highlighted through post-event surveys, experimental and numerical studies. Although many innovative solutions have been proposed, especially in the last decades, many aspects of these systems are object of ongoing or future studies. The ductile infills with sliding joints have been currently investigated by different researchers starting from experimental tests and using the test outcomes to calibrate and create finite element models with the aim to perform parametric analysis and define the local and global interaction with the structure. Moreover, the innovative infills with sliding joints have shown a completely different in-plane behavior with respect to the non-ductile ones. Since the creation of the diagonal strut is avoided and the shear sliding mechanisms fostered in predefined sliding joints, the interaction between the masonry panel and the RC members represents novelty with respect to the "traditional" rigidly attached masonry solutions. Within the present paper the results of a numerical model calibrated according to in-plane experimental tests are presented and the local interaction between the RC structural member and the innovative ductile infill with sliding joints is discussed. The study adopts a validated finite element model approach to an experimental campaign that has never been simulated through detailed FEMs and compares the numerical results with the experimental results related to the local effects.*

**Keywords:** Local effects, infill-frame interaction, innovative infills, ductile infills, sliding joints, fem modeling of infills.

ISSN:2623-3347 
Peer-review under responsibility of the organizing committee of COMPDYN 2021.
doi:10.7712/120121.8533.19421

## 1 INTRODUCTION

The seismic vulnerability of rigidly attached masonry infills, also called non-ductile infills, has been repeatedly highlighted through recent post-event surveys (*i.e.*, [1],[2],[3],[4]). Several problems have been observed such as the in-plane/out-of-plane interaction in the seismic response of these non-structural elements (Figure 1a), the global influence in the overall seismic behaviour of the structure and the structural damages caused by local interaction between the masonry panels and the structural members (Figure 1b). The seismic behaviour of non-ductile masonry infills has been studied also experimentally and numerically into many researches that had different goals such as, the infill/structural global interaction ([5],[6],[7]), the in-plane behaviour ([8],[9]), the out-of-plane response ([10],[11],[12]). The in-plane/out-of-plane interaction ([13],[14],[15]), the economic evaluation of the expected annual losses ([16],[17]) and the local interaction between the infill and the structural members ([18],[19],[20]) as, for example, shown in Figure 2, were investigate as well.

(a) (b)

Figure 1: (a) Infill damage and collapse due to in-plane and out-of-plane behaviour during the Central Italy earthquake 2016 ([3]), (b) Focus on the local damages on RC members due to the infill-structure local interaction ([2]).

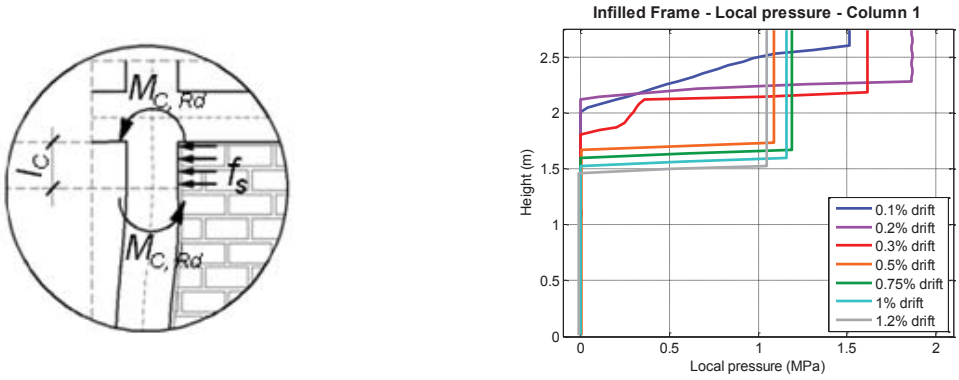


(a) (b)

Figure 2: (a) Local effects on a non-ductile infill to the adjacent column ([20]); (b) Example of local pressure at different drift on the RC columns due to the presence of a non-ductile infill made of AAC units ([20]).

The aforementioned issues have recently encouraged the research and the industry in developing innovative infills that can be generally classified into three categories: the enhanced infills ([21],[22],[23],[24]), the panels uncoupled from the frame ([25],[26]) and the ductile infills ([27],[28],[29],[30],[31]). The latter innovative infill typology, that has been recently proposed and studied both experimentally and numerically, is object of ongoing and future studies. The infill with sliding joints, which are investigated in this work, are classified as ductile infills. The innovative infills with sliding joints have shown a completely different in-plane behaviour with

respect to the non-ductile ones [32]. Since the creation of the diagonal strut is avoided and the shear sliding mechanisms fostered in predefined sliding joints, the interaction between the masonry panel and the RC members represents a novelty with respect to the "traditional" rigidly attached masonry solutions.

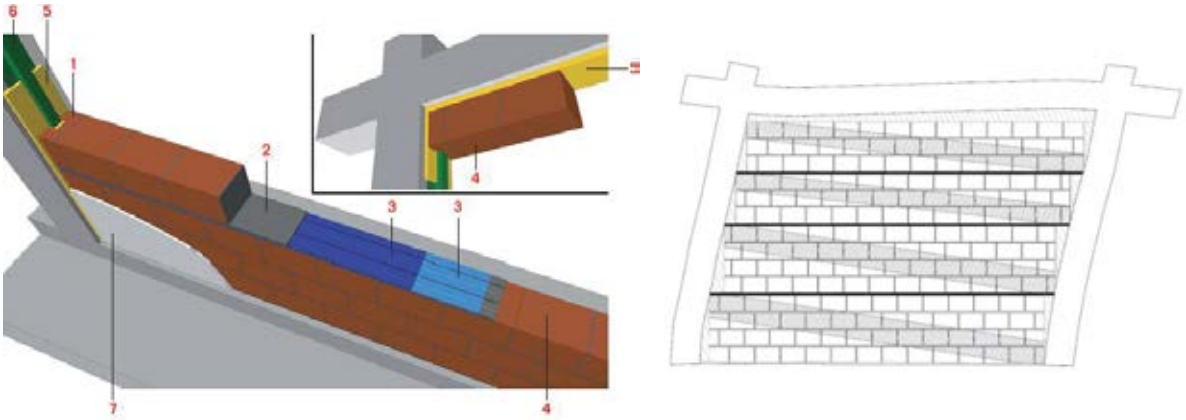


(a) (b)

Figure 3: (a) Details of the innovative masonry infill with sliding joints: 1. C-shape units; 2. mortar bed-joints; 3. (b) sliding joints; 4. clay units; 5. interface joints; 6. shear keys; 7. plaster ([28],[29]); (b) Idealization of the compressed strut in the case of ductile infill with sliding joints ([28]).

Within the present paper the results of a numerical model calibrated according to in-plane experimental tests are presented and the local interaction between the reinforced concrete structural member and the innovative ductile infill with sliding joints is discussed. The study adopts a validated finite element model approach ([33]) extended to an experimental campaign ([28]) that has never been simulated through detailed FEMs and compares the numerical results with the experimental ones related to the local effects.

## 2 SPECIMEN DESCRIPTION AND INSTRUMENTATION

At the Department of Civil Engineering and Architecture and at the Eucentre Foundation, within the European FP7 "INSYSME" project, a ductile seismic resistant masonry infill with sliding-joints ([28] and [29]) with original details has been conceived, based on the conceptual design proposed in Preti *et al.* [34]. The engineered system reduces the interaction between the structure and the infill in the in-plane direction by facilitating the shear-sliding damage in specific previously designed elements corresponding to the sliding joints. The infill is subdivided into four horizontal subpanels that can mutually slide through properly conformed sliding joints. Moreover, the interface between the masonry subpanels and the reinforced concrete is filled with a deformable mortar to decrease the stress concentration. The unreinforced masonry used in the subpanels of the infill is realized with vertically perforated lightweight clay units and general-purpose 1 cm thick mortar bed- and head-joints.

The reference experimental campaign has included test on characterization on every material (concrete, reinforcement, mortar, clay units and masonry), in-plane pseudo-static cyclic tests (called IPL) on fully and partially infilled (with a central opening) full scale one-storey one-bay reinforced concrete frames. The infill without opening has been tested also at "high-velocity" (called IPH) to study the behaviour of the sliding joints subjected to dynamic actions. Subsequently, the same specimens have been tested dynamically out-of-plane on a shaking table to investigate the out-of-plane response. Finally, a dynamic test on a shaking table on a prototype 2-storeys 5-bays building has been carried out. The in-plane response is presented by Morandi

*et al.* [28], the out-of-plane experimental behaviour is discussed in Milanesi *et al.* [29], whereas the building test is presented in Manzini *et al.* [35].

The full infill, named TSJ1, had a length of 4.22 m and a height of 2.95 m, and the reinforced concrete members have a square section with base/height of 35 cm (Figure 4). The specimen design, that aimed to represent a part of a realistic full-scale reinforced frame structure, is detailed in other works ([9] and [28]).

The experimental displacements and deformations occurred during the in-plane tests have been measured through 45 displacement transducers (linear potentiometers) (Figure 5a). The ones numerated between 30 and 44 are located at the panel/column interface to measure the compression of the deformable mortar joint or the detachment of the subpanel with the reinforced concrete column (Figure 5b). Each subpanel has 2 potentiometers for each masonry/column interface, being one at the top and the other at the bottom of the subpanel.

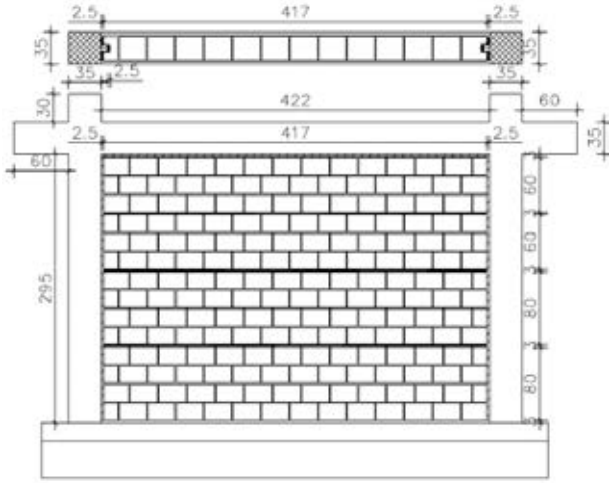


Figure 4: Layout of the fully infilled specimen represented without plaster ([28]).

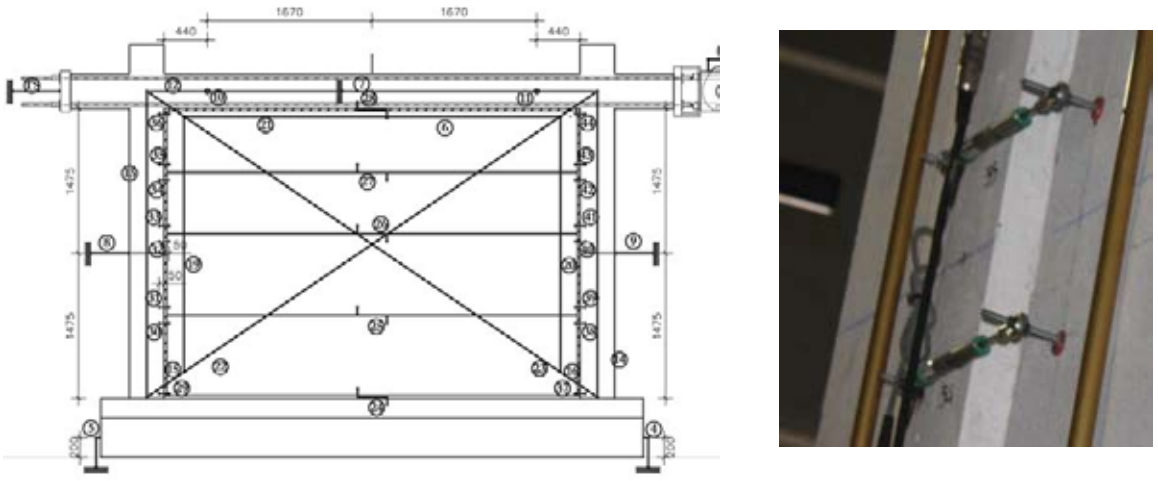


(a) (b)

Figure 5: (a) Sketch of the linear potentiometer installed in the specimen during the in-plane cyclic test; (b) Detail of the potentiometer 34 and 35 installed to monitor the subpanel/column local interaction.

## 3 EXPERIMENTAL RESULTS

The force-displacement hysteretic curves and the corresponding envelopes for each cycle of the fully infilled configuration (TSJ1) are reported in Figure 6a, whereas the results of the bare frame specimen (called TNT) are shown in Figure 6b. The TNT specimen has been taken as

reference for a proper evaluation of the infill contribution and it has been tested in a previous experimental campaign ([9]).

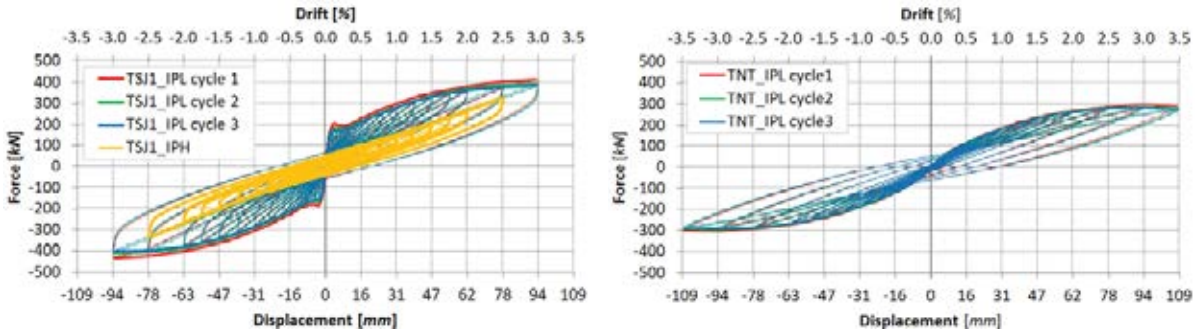


Figure 6: Experimental force-displacement cyclic and envelopes curves of (a) specimen TSJ1, fully infilled and (b) bare frame.

The damage related to the in-plane tests, which is detailed in Morandi *et al.* [28], can be summarized to horizontal cracks corresponding to the sliding mechanism of the sliding joints starting from low levels of drift (from 0.20%), sub-horizontal flexural and light diagonal cracks in the upper and bottom part of the reinforced concrete columns due to the in-plane deformation of the structural frame (at about 1.00-1.25%), detachment of small area of plaster in corner of the subpanels (2.00%) and spalling of the concrete cover at the bottom of the columns (3.00%). At the subpanel/column interface, the occurrence of the sliding mechanism in the engineered sliding joints has created a contact area and a detached portion for every subpanel due to the deformation of the reinforced concrete frame respect to the infill (Figure 7).

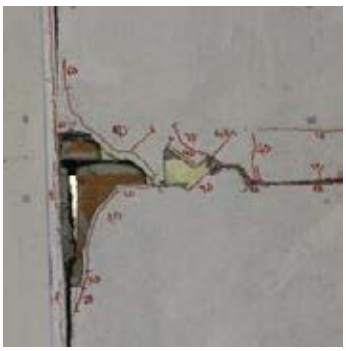

Figure 7: Focus of the masonry/column interface joint at the max imposed in-plane drift of 3.00%.

As aforementioned, the experimental campaign has included also a comprehensive mechanical characterization of the materials. The masonry has been therefore characterized through vertical, horizontal, and diagonal compressive strength tests, flexural pure bending tests, and tests on triplets to determine the initial shear resistance and the friction coefficient of the mortar bed-joints and the sliding joints. All tests of characterization on masonry have been conducted on specimens with and without plaster in order to evaluate its influence for each resistance. In the present work only the horizontal compressive resistance of the masonry (Figure 8a) and the shear tests on masonry triplets to characterize the cohesion and the friction coefficient of the mortar bed-joints and the sliding joints (Figure 8b) have been consider.

Figure 8c reports the results of the triplet tests on masonry for the sliding joints, for the mortar bed-joint with and without plaster. The stress-strain curve obtained from the horizontal compressive tests is reported in Figure 12b.

Furthermore, the deformable interface mortar (called "deformable mortar" in the following) placed between the masonry subpanels and the structural member has been characterized in several ways: by testing mortar prisms in compression (Figure 9a), mortar pads (Figure 9b) to investigate the influence of the dimension and by the replicating the whole interface region also including the steel omega element and the C-shape clay unit (Figure 9c). The results, that are reported in Figure 13a, highlight the lack of a common curve and the necessity to make some assumption regarding the compressive behaviour of this material.

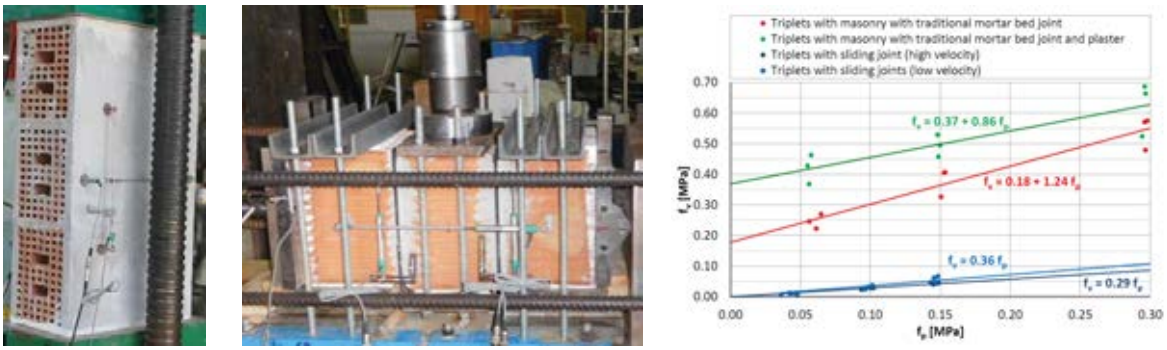


(a) (b) (c)

Figure 8: Picture of the tests of characterization to determine the (a) horizontal resistance of the masonry, (b) friction coefficient of the sliding joints. (c) Results of the initial shear resistance of the masonry triplets.

(a) (b) (c)

Figure 9: Picture of the tests of characterization for the deformable mortar at the panel/frame interface (a) test on mortar prism; (b) test on mortar pad; (c) replication of the whole contact system.

## 4 MODELING DESCRIPTION

The modelling technique here adopted to interpret the test response is based on the approach proposed in several studies ([36][37],[38]) and specified for sliding joint infill in Bolis *et al.* ([33]). The specific configuration of the infill with sliding joints and the layer of deformable mortar interposed at the frame to masonry interface, is modelled with interface and smeared-crack elements, respectively. For the specific specimen under consideration here, the deformable mortar is modelled assuming a simplified linear response calibrated on the mechanical characterization tests.

The model is a two-dimensional plane-stress finite element model implemented using the FEAP ([39]) environment.

The modelling scheme of reinforced concrete columns, beam members and masonry infill ([38]) are reported in Figure 10. The sliding joints are modelled using interface elements; the lateral deformable mortar joints are simulated using a smeared-crack element directly connected to the nearest reinforced concrete member on one side and through an interface element to the adjoining masonry subpanel. Unlike the model proposed in Bolis *et al.* ([33]) the base

joint is modelled like the horizontal mortar joints and the top deformable mortar joint between the masonry infill and the beam is modelled like the lateral vertical joints (Figure 11).

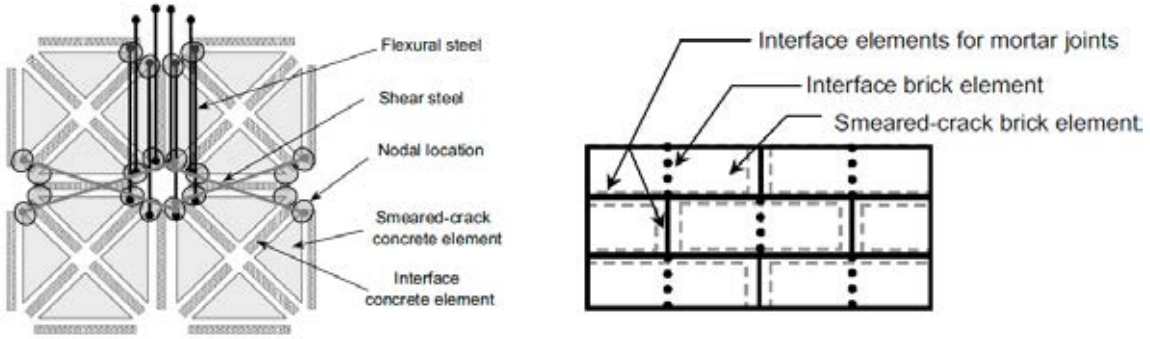


RC members Masonry infill panel

Figure 10: Finite element discretization reprinted from Stavridis and Shing ([38]).

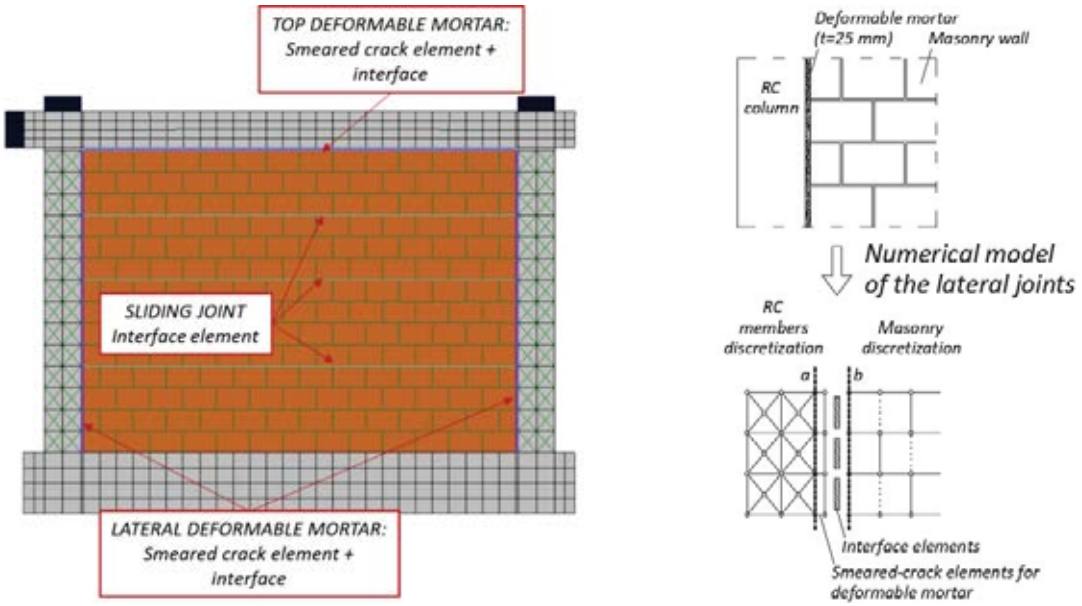


(a) (b)

Figure 11: (a) Infill frame mesh and detail of the sliding and contact joints; (b) detail of the contact joint modeling

## 4.1 Parameter calibration

The model parameters are calibrated as proposed in Stavridis and Shing ([38]) and Bolis *et al.* ([33]), referring to experimental tests performed on subassembly and to literature references. The main parameters are reported in Table 1 and Table 2.

| Material | SMEARED-CRACK ELEMENTS | | | | | |
|---|---|---|---|---|---|---|
| | E [MPa] | G [MPa] | ν [-] | t [mm] | $f_c$ [MPa] | $f_t$ [MPa] |
| Concrete | 25000 | 10417 | 0.20 | 350 | 37 | 1 |
| Masonry | 2600 | 1150 | 0.13 | 250 | 2.9 | 0.6 |
| Deformable Mortar top | 5 | 2 | 0.38 | 100 | 10.0 | 2.0 |
| Deformable Mortar lateral | 8 | 2.9 | 0.38 | 250 | 10.0 | 2.0 |

Table 1: Main parameters adopted for the smeared-crack elements.

The comparison between the numerical and experimental results of the main calibration tests are reported in the following Figure 12 and Figure 13.

Lateral and top deformable mortar joints are modelled using smeared-crack elements calibrated to have an elastic behaviour in the range of deformation of interest. The elastic modulus of the lateral deformable mortar is calibrated to obtain a stress strain curve secant to the experimental on in the range of strain of 15-20%, which corresponds to the peak strain level measured in the experiment on the infilled frame structure at drift level of about 2.0%. In Figure 13a is reported the comparison between the assumed elastic curve and the experimental stress-strain ones obtained in the characterization tests. A similar approach is adopted for the top deformable mortar, accounting for a lower strain demand during the test.

The interface elements representing the sliding joints are calibrated fitting the residual yield surface to the experimental results. The initial yield surface is obtained by shifting upward the residual one calibrated to the test of the only sliding joint to consider the effect of the reduced plaster thickness at the sliding joint location.

| Material | INTERFACE ELEMENTS | | | | | |
|---|---|---|---|---|---|---|
| | $s_0$ [MPa] | $\mu_0$ [-] | $\mu_r$ [-] | $r_0$ [MPa] | $r_r$ [MPa] | t [mm] |
| Bed joints | 0.45 | 0.88 | 0.75 | 0.005 | 0.005 | 250 |
| Brick head joints | 0.70 | 1.00 | 0.80 | 0.28 | 0.21 | 250 |
| Mortar vertical joints | 0.90 | 0.862 | 0.75 | 0.005 | 0.005 | 250 |
| Concrete joints | 1.00 | 0.90 | 0.70 | 0.25 | 0.20 | 350 |
| Lateral joints | 0.05 | 0.50 | 0.45 | 0.10 | 0.10 | 250 |
| Top joint | 0.05 | 0.25 | 0.20 | 0.10 | 0.10 | 250 |
| Sliding joints | 0.15 | 0.361 | 0.361 | 0.02 | 0.02 | 250 |

Table 2: Main parameters adopted for the interface elements.

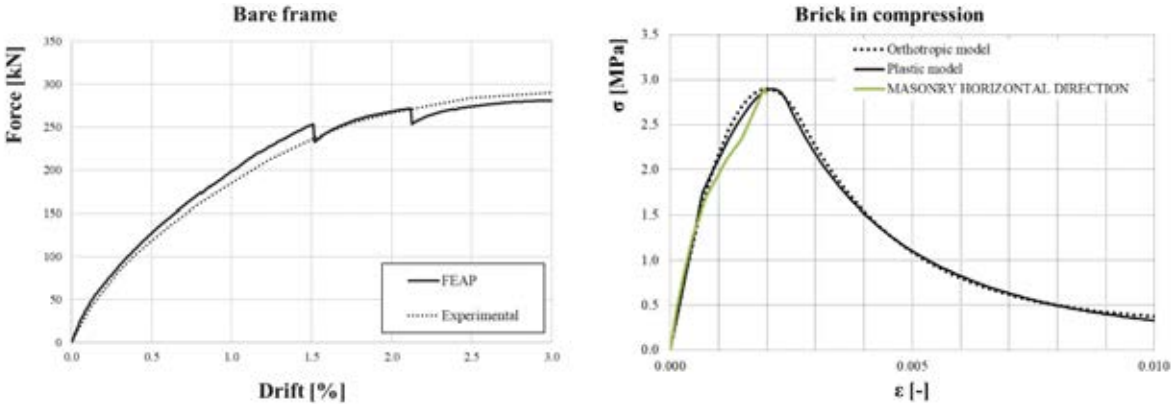


(a) (b)

Figure 12: (a) Numerical and experimental results for bare frame; (b) Comparison of experimental test of characterization and numerical simulation of the stress-strain response of the masonry in the horizontal direction.

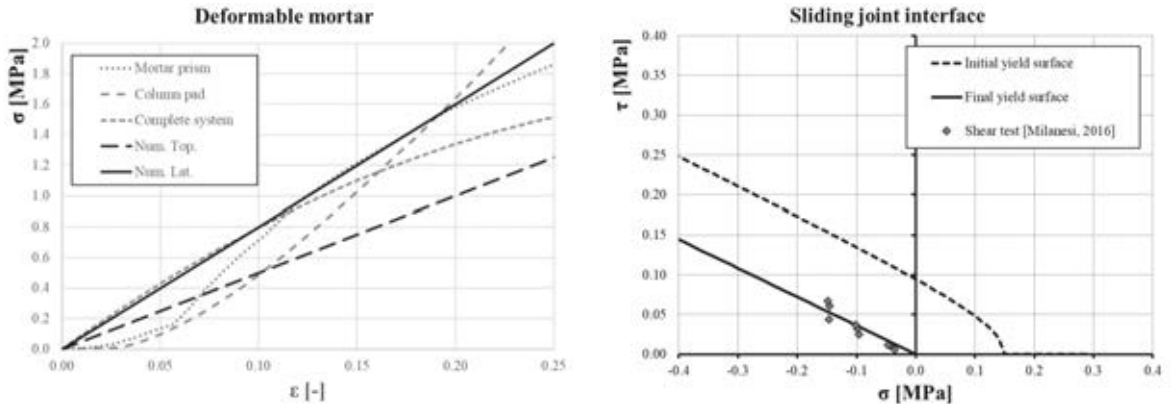


(a) (b)

Figure 13: (a) Comparison of the stress-strain experimental response of deformable mortar test and the elastic model adopted in the numerical model; (b) Comparison of the shear stress–compressive stress experimental response and the numerical model adopted.

# 5 NUMERICAL AND EXPERIMENTAL RESULTS COMPARISON

## 5.1 Global behavior

In Figure 14 the monotonical hysteresis is reported in terms of force applied at the top of the frame versus the displacement for both positive and negative in-plane loading, for experimental and numerical results. The experimental curve considered is the envelope of positive (push) and negative (pull) displacements of the cyclic tests conducted. Given the symmetry of the model the same numerical behaviour is considered for each load direction.

In both direction of loading the initial stiffness is well captured, whereas the initial peak of resistance is slightly underestimated, probably due to the uncertainties in the evaluation of the reduced thickness of the plaster over the sliding joints. As the drift increases, the horizontal joints start sliding and the behaviour exhibits a stiffness decay. The peak resistance reached in the simulation is slightly higher than the experimental ones, with an overestimation lower than 10% and more evident in the positive direction.

The quality of the numerical simulation can be better evaluated by focusing on the local response of the masonry/column deformable mortar joints shown in Figure 15.

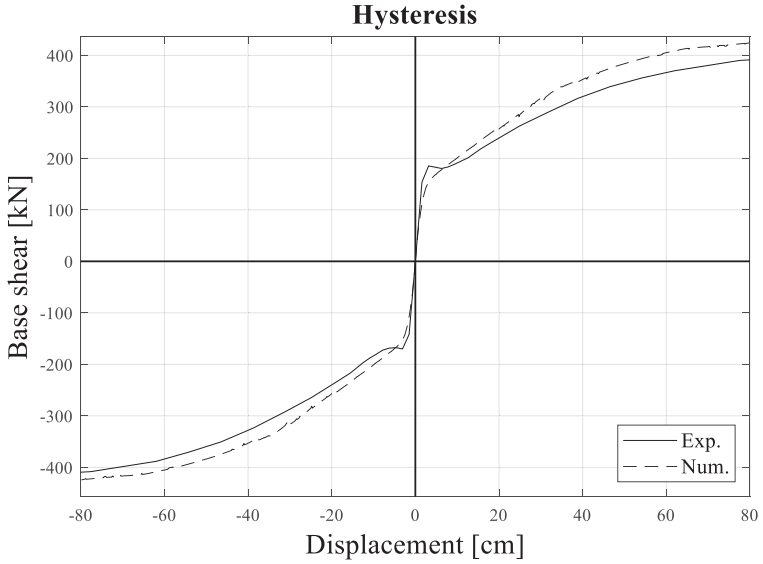


Figure 14: Experimental and numerical hysteresis.

## 5.2 Local behavior

The comparison between experimental and numerical local deformation of the lateral joints along the frame height is herein presented. Given that the masonry is two order of magnitude stiffer than the deformable mortar, therefore, the local experimental deformations are estimated assuming that the displacement read by the potentiometer is localized in the deformable mortar joint only. The ratio between the displacement output and the thickness of the interface mortar joint, equal to 25 mm, has been assumed as the experimental strain of the deformable material. Since there are two potentiometers for each subpanel, the deformation profile of each of them is obtained considering the line interpolating the two values.

Numerically, the deformation profile is obtained directly from the difference of displacement between the masonry node and the concrete node near the lateral joints (alignment “a” and “b” in Figure 11).

It is important noting that the profile given represents the average strain in the lateral joint and it is not the specific deformation of the mortar. However, it can be assumed as an acceptable estimation of the compression strain level.

For all drift level the compression area is well captured. At 2.00% of drift the maximum compressive strain is approximately equal to 20%, confirming the strain level considered for the deformable mortar elastic modulus calibration.

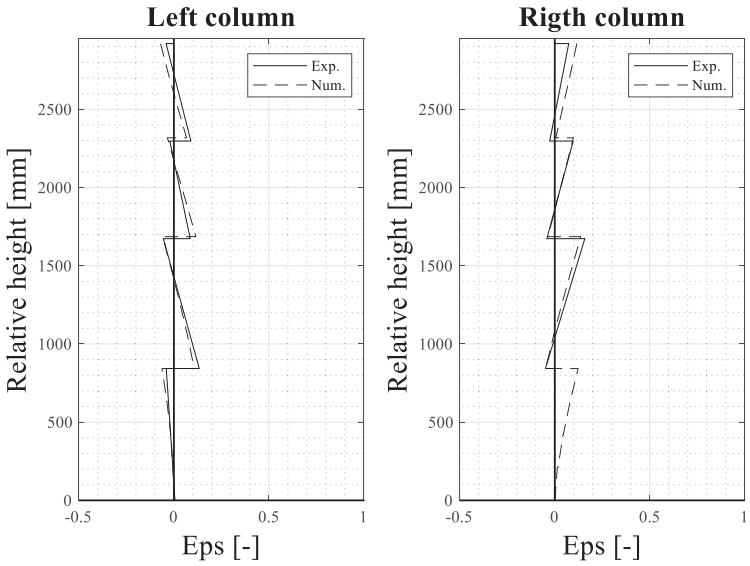


Lateral joints deformation for each column at 0.5% Drift

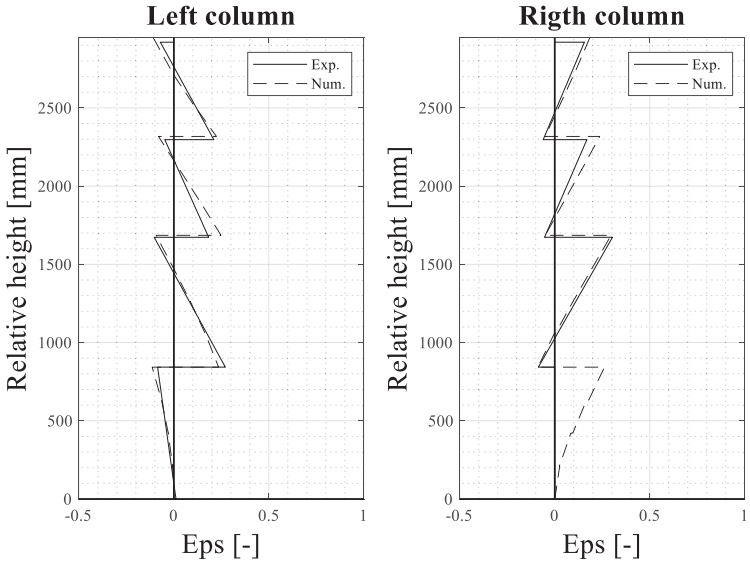


Lateral joints deformation for each column at 1.0% Drift

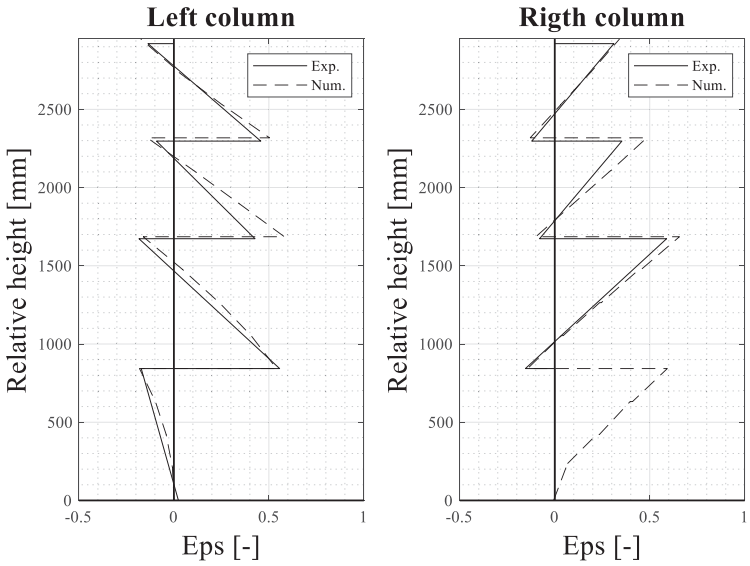


Lateral joints deformation for each column at 2.0% Drift

Figure 15: Lateral joint deformation for each column at different levels of drifts.

## 6 CONCLUSIONS

The recent outcomes from different post-seismic inspections and experimental and numerical studies on infills have identified many issues on non-ductile rigidly attached masonry infills. Three categories of innovative solutions have been proposed to improve the seismic response of these non-structural elements, being the ductile infills with sliding or deformable joints the latest respect to the others that aim to enhance the masonry and to uncouple the panel from the structure. The innovative ductile infill system with sliding joints is object of ongoing and future investigation to improve the knowledge about this new infill typology.

The experimental tests summarized in the present work ([28]) have been integrated with a detailed finite element model that has been previously adopted for a similar infill ([27],[33]). The model is a two-dimensional plane-stress finite element model implemented using the FEAP ([39]) environment. The results of the numerical simulation of the experimental in-plane test on the fully infilled solution has shown the capability of the model to capture both the overall behaviour and the local deformation located in the deformable mortar at the masonry/column interface. Moreover, one future development of the present study will be the computation of the local forces that occur in every subpanel/column contact area starting from the strain plots of the interface deformable mortar discussed herein.

Finally, the experimental evidence and the numerical results highlight the different in-plane behaviour of the infill typology and their new local interaction with the structure respect to non-ductile “traditional” systems, therefore new design provisions for the shear verification of the structural members could represent another future development of the present study.

## ACKNOWLEDGEMENT

The experimental campaign presented in this work has been conducted thanks to the financial support of the European Commission within the project INSYSME “INnovative SYStems for earthquake resistant Masonry Enclosures in rc buildings”, grant FP7-SME-2013-2-GA606229, 2013-2016 is acknowledged. ANDIL and its associated companies, and RUREDIL spa are gratefully acknowledged as industrial partners of the INSYSME project, where the University of Pavia has also been partner. The contribution of Capaccioli srl for the supply of the sliding joints is acknowledged. The numerical part and the study of the local effects have been

whereas conducted within the framework of DPC/ReLUIS project 2019-2021, WP10, where both the University of Pavia and the University of Brescia are involved.

## REFERENCES

[1] Manzini, C.F., Morandi, P., 2012. Rapporto preliminare sulle prestazioni ed i danneggiameti agli edifici in muratura portante moderni a seguito degli eventi sismici emiliani del 2012 (in Italian), Eucentre, www.eqclearinghouse.org/2012-05-20-italy/.

[2] Parisi F., De Luca F., Petruzzelli F., De Risi R., Chioccarelli E.,Iervolino I., 2012. *Field inspection after the May 20th and 29th 2012 Emilia-Romagna earthquakes*, available at http://www.reluis.it.

[3] Fragomeli, A., Galasco, A., Graziotti, F., Guerrini, G., Kallioras, S., Magenes, G., Malomo, D., Mandirola, M., Manzini, C.F., Marchesi, B., Milanesi, R.R., Morandi, P., Penna, A., Rossi, A., Rosti, A., Rota, M., Senaldi, I., Tomassetti, U., Cattari, S.,da Porto, F., Sorrentino, L., 2017. Comportamento degli edifici in muratura nella sequenza sismica dell'Italia centrale del 2016 – Parte 1: Quadro generale (in Italian), *Progettazione sismica*, **8**(2), 49-77.

[4] Fikri, R., Dizhur, D., Walsh, K., Ingham, J., 2019. Seismic performance of Reinforced Concrete Frame with Masonry Infill buildings in the 2010/2011 Canterbury, New Zealand earthquake, Bulletinf of Earthquake Engineering, **17**, 737-757.

[5] Fiore, A., Netti, A., Monaco, P., 2012. The influence of masonry infill on the seismic behaviour of RC frame buildings. *Engineering Structures*, **44**, 133-145.

[6] Ricci, P., De Risi, M.T., Verderame, G.M., Manfredi G., 2013. Influence of infill distribution and design typology on seismic performance of low- and mid-rise RC buildings, *Bulletin of Earthquake Engineering*, **11**, 1585-1616

[7] Pantò, B., Caliò, I., Lourenço, P.B., 2017. Seismic safety evaluation of reinforced concrete masonry infilled frames using macro modelling approach, *Bulletin of Earthquake Engineering*, **15**, 3871-3895.

[8] Mehrabi, A.b., Shing, P.B., 1997. Finite element modeling of masonry-infilled RC frames, *Journal of Structural Engineering*, **123**(5), 604-613.

[9] Morandi, P., Hak, S., Magenes, G., 2018. Performance-based interpretation of in-plane cyclic tests on RC frames with strong masonry infills, *Engineering Structures*, **155**, 503-521.

[10] Abrams, D.P., Angel, R., Uzarski, J., 1996. Out-of-plane strength of unreinforced masonry infill panels, *Earthquake Spectra*, **12**(4): 825-844.

[11] Palieraki, V., Zeris, C., Vintzileou, E., Adami, C.E., 2018. In-plane and out-of-plane response of currently constructed masonry infills, *Engineering Structures*, **177**, 103-116.

[12] Milanesi, R.R., Morandi, P., Hak, S., Magenes, G., 2021. A new prospective towards out-of-plane verifications of URM infills, *Proc. 14th Canadian Masonry Symposium*, 16-19 May 2021, Montreal, Canada.

[13] Calvi, G.M., Bolognini, D., 2001. Seismic response of RC frames infilled with weakly reinforced masonry panels, *Journal of Earthquake Engineering*, **5**(2), 153-185.

[14] Di Trapani, F., Shing, P.B., Cavaleri, L., 2017. Macroelement model for in-plane and out-of-plane responses of masonry infills in frame structures, *Journal of Structural Engineering*, **144**(2):04017198.

[15] Ricci, P., Di Domenico, M., Verderame, G.M., 2020. Effects of the in-plane/out-of-plane interaction in URM infills on the seismic performance of RC buildings designed to Eurocodes, *Journal of Earthquake Engineering*, DOI: 10.1080/13632469.2020.1733137

[16] Di Trapani, F., Bolis, V., Basone, F., Preti, M., 2020. Seismic reliability and loss assessment of RC frame structures with traditional and innovative masonry infills. *Engineering Structures*, **208**, 110306, 2020.

[17] Rossi, A., Morandi, P., R.R., Magenes, G., 2021. A novel approach for the evaluation of of the economical losses to seismic actions on RC buildings with masonry infills, *Soil Dynamics and Earthquake Engineering*, 145, 106722, doi 10.1016/j.soildyn.2021.106722.

[18] Crisafulli, F.J., Carr, A.J., Park, R., 2000. Analytical Modeling of Infilled Frame Structures - A General Review, *Bulletin of the New Zealand Society for Earthquake Engineering*, **33**.

[19] Cavaleri, L., Di Trapani, G., 2015. Prediction of the additional shear action on frame members due to infills. *Bulletin of Earthquake Engineering*, **13**, 1425-1454.

[20] Milanesi, R.R., Morandi, P., Magenes, G., 2018. Local effects on RC frames induced by AAC masonry infills through FEM simulation of in-plane tests, *Bulletin of Earthquake Engineering*, **16**, 4053-4080.

[21] Valluzzi, M.R., da Porto, F., Garbin, E., Panizza, M., 2014. Out-of-plane behaviour of infill masonry panels strengthened with composite materials, *Materials and structures*, **47**(12), 2131-2145.

[22] Verderame, G.M., Balsamo, A., Ricci, P., Di Domenico, M., Maddaloni, G., 2019. Experimental assessment of the out-of-plane response of strengthned one-way spanning masonry infill walls, *Composite Structures*, **230**, 111503.

[23] Pohoryles, D.A., Bournas, D.A., 2020. Seismic retrofit of infilled Rc frames with textile reinforced mortars: state-of-the-art review and analytical modelling, *Composites Part B*, **183**, 107702.

[24] Furtado, A., Rodrigues, H., Arêde, A., Melo, J., Varum, H., 2020, The use of textile reinforced mortar as a strengthening technique for the infill walls out-of-plane behaviour, *Composite Structures*, doi: https://doi.org/10.1016/j.compstruct.2020.113029

[25] Marinkovic, M., Butenweg, C., 2019. Innovative decoupling system for the seismic protection of masonry infill walls in reinforced concrete frames, *Engineering Structures*, **197**, 109435.

[26] Binici, B., Canbay, E., Aldermir, A., Demirel, I.O., Uzgan, U., Eryurtlu, Z., Bulbul, K., Yakut, A., 2019. Seismic behaviour and improvement of autoclaved aerated concrete infill walls, *Engineering Structures*, **193**, 68-81.

[27] Preti, M., Bettini, N., Plizzari, G., 2012. Infill Walls with Sliding Joints to Limit Infill-Frame Seismic Interaction: Large-Scale Experimental Test, *Journal of Earthquake Engineering*, **16**(1), 125–141.

[28] Morandi, P., Milanesi, R.R., Magenes, G., 2018. Innovative solution for seismic-resistant masonry infills with sliding joints: in-plane experimental performance, *Engineering Structures*, **176**, 719-733.

[29] Milanesi, R.R., Morandi, P., Manzini, C.F., Albanesi, L., Magenes, G., 2020. Out-of-plane response of an innovative masonry infill with sliding joints from shaking table tests. *Journal of Earthquake Engineering*. DOI: 10.1080/11632469.2020.1739173.

[30] Cheng, X., Zou, Z., Zhu, Z., Zhai, S., Yuan, S., Mo, Y., Chen, W., He, J., 2020. A new construction technology suitable for frame partitioned infill walls with sliding nodes and large openings: test results, *Construction and Building Materials*, **258**, 119644.

[31] Totoev, Y.Z., Al Harthy, A., 2016. Semi interlocking masonry as infill wall system for earthquake resistant buildings: a review. *The Journal of Engineering Research* (TJER), **13**, 33-41.

[32] Preti, M., Bolis, V., Stavridis, A., 2017. Seismic infill-frame interaction of masonry walls partitioned with horizontal sliding joints: analysis and simplified modelling, *Journal of Earthquake Engineering*, DOI: 10.1080/13632469.2017.1387195.

[33] Bolis, V., Stavridis, A., Preti, M., 2017. Numerical Investigation of the In-Plane Performance of Masonry-Infilled RC Frames with Sliding Subpanels, *Journal of Structural Engineering*, **143**(2), 04016168. doi: 10.1061/(ASCE)ST.1943-541X.0001651

[34] Preti, M., Migliorati, L., Giuriani, E., 2015. Experimental testing of engineered masonry infill walls for post-earthquake structural damage control, *Bulletin of Earthquake Engineering*, **13**(7), 2029–2049.

[35] Manzini, C.F., Morandi, P., Milanesi, R.R., Magenes, G., 2018. Shaking-table test on a two-storey RC framed structured with innovative infills with sliding joints, *Proc. 16th ECEE*, 18-21 June 2018, Thessaloniki, Greece.

[36] Lotfi, H.R., Shing, P.B., 1991. An appraisal of smeared crack models for masonry shear wall analysis, *Computers & Structures*, **41**(3), 413–425, doi: 10.1016/0045-7949(91)90134-8.

[37] Lotfi, H.R., Shing, P.B., 1994. Interface Model Applied to Fracture of Masonry Structures, *Journal of Structural Engineering*, **120**(1), 63–80, doi: 10.1061/(ASCE)0733-9445(1994)120:1(63).

[38] Stavridis, A., Shing, P.B., 2010. Finite-Element Modeling of Nonlinear Behavior of Masonry-Infilled RC Frames, *J. Struct. Eng.*, **136**(3), 285–296, doi: 10.1061/(ASCE)ST.1943-541X.116.

[39] Taylor, R.L., Govindjee, S., *FEAP - - A Finite Element Analysis Program*, p. 705.